

Design and Analysis of A Novel Miniaturized Dual-Band Omnidirectional Antenna for WiFi Applications

Ya-Bing Yang^{1, 2, *}, Fu-Shun Zhang¹, Yun-Qi Zhang³, and Xu-Ping Li³

Abstract—In this article, a novel dual-band omnidirectional antenna for WiFi applications is presented and investigated. The proposed antenna is mainly composed of two pairs of half-wavelength dipoles with different lengths. It is fed by a microstrip balun, which provides a good impedance matching for desired dual-band operation. The dimension of the proposed antenna is only $50\text{ mm} \times 10\text{ mm} \times 1\text{ mm}$ ($0.4\lambda_0 \times 0.08\lambda_0 \times 0.008\lambda_0$, and λ_0 is the wavelength of 2.4 GHz). The performance study of this dual-band omnidirectional antenna with different geometric parameters has been conducted. The final design is fabricated and measured, and the results exhibit a good impedance bandwidth of approximately 19.2% for $|S_{11}| \leq -10\text{ dB}$ ranging from 2.24 to 2.70 GHz centered at 2.4 GHz, and over 17.4% for $|S_{11}| \leq -10\text{ dB}$ ranging from 4.73 to 5.6 GHz centered at 5.0 GHz. This antenna also has a stable gain of $2.09 \sim 2.87\text{ dBi}$ and omnidirectional radiation patterns over the whole operating band. Dual-band coverage, stable omnidirectional radiation performance, simple structure, and miniaturized dimension make this antenna an excellent candidate for WiFi applications.

1. INTRODUCTION

In the last few decades, omnidirectional antenna has drawn considerable attention especially for wireless communication, as it has the advantage of full coverage on the horizontal, ensuring reliable connectivity with a high degree of mobility, supporting free alignment between the wireless router and the mobile devices. Wireless fidelity (WiFi), which operates in the 2.4 GHz and 5.0 GHz industrial, scientific, and medical (ISM) bands, is a superset of the IEEE 802.11 a/b/g/n standards for WLAN communications. A WiFi router connects to the network via an access point at the respective frequency ranges from 2.4 to 2.485 GHz as well as 4.9 ~ 5.1 GHz, 5.15 ~ 5.35 GHz, 5.47 ~ 5.725 GHz and 5.725 ~ 5.85 GHz [1, 2]. Antennas with dual-band or multi-band characteristics for various standards and protocols have become necessary. For realizing the dual-band omnidirectional operation, it is common to integrate two antennas together with the same feeding network or diplexer. An improvement has been made using three polygonal radiation patches with three equally spaced legs shorted to the ground plane [3]. Similar works have been reported in [4, 5]. Such a type of antenna is confirmed of wide bandwidth for dual-band operation, but the size is usually too large for WiFi devices. In [6], a dual-band monopole antenna using substrate-integrated suspended line technology for 2.4/5.2 GHz WLAN application is proposed. In spite of stable omnidirectional radiation patterns, the high cost and complicated structure are not suitable for practical use. A novel dual-polarized dual-band omnidirectional antenna designed for GPS and WLAN applications is obtained. Although the profile is low, the diameter is still too large [7]. Besides, dielectric resonator antenna (DRA) has been extensively investigated, which may become a good candidate for dual-band omnidirectional operations [8] while the dimension is the key problem.

Received 8 May 2020, Accepted 1 July 2020, Scheduled 11 July 2020

* Corresponding author: Ya-Bing Yang (antenna206@163.com).

¹ Key Laboratory of Antennas and Microwave Technology, Xidian University, Xi'an, Shaanxi 710071, China. ² Xi'an Electronic Engineering Research Institute, Xi'an, Shaanxi 710100, China. ³ School of Electronic Engineering, Xi'an University of Posts & Telecommunications, Xi'an, Shaanxi 710121, China.

Some other researches on dual-band omnidirectional antenna have realized the miniaturized size. For example, a dual-ISM-band antenna using a spiral structure with parasitic element is also compact in size [9]. In [10], a stacked configuration is used for dual-band operation at 2.5 GHz and 3.5 GHz. A comparison between previous works in the literature and the designed antenna is summarized in Table 1. Here, λ_0 is the wavelength of the lower frequency band. The table shows that the proposed antenna has the advantages of smaller dimension and better ellipticity in the azimuth plane.

Table 1. Comparison to previous antennas.

	Overall Size (λ_0)	Ellipticity (dB)	Peak Gain (dBi)
[3]	$1.05 \times 1.05 \times 0.59$	2.5	3
[4]	$0.24 \times 0.24 \times 0.34$	2	5.2
[8]	$0.32 \times 0.08 \times 0.01$	NOT GIVEN	2.25
[9]	$0.5 \times 0.25 \times 0.175$	4.5	1.45
Pro.	$0.4 \times 0.08 \times 0.008$	2.1	2.09 ~ 2.87

In this article, a novel miniaturized dual-band omnidirectional antenna for WiFi applications is studied. By integrating two pairs of dipoles, the proposed antenna shows perfect dual-band characteristics. The design and analysis for the proposed antenna are presented in Section 2. Section 3 discusses the measured and simulated results. Section 4 is a brief conclusion for this letter.

2. ANTENNA DESIGN

The proposed miniaturized dual-band omnidirectional antenna operates at both 2.4 GHz and 5.0 GHz bands, and the half-wavelength dipole with omnidirectional radiation pattern is considered as the basic structure. The low band dipole is presented in Figure 1(a), while the high band dipole is depicted in Figure 1(b). These two basic dipoles are combined by a parallel two-wire transmission line, and the width of the transmission line needs to be optimized for impedance matching in the design. Besides, the

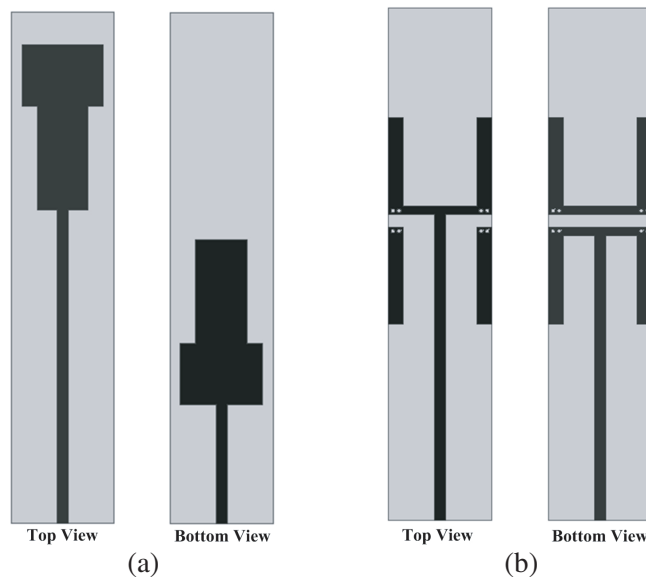


Figure 1. The basic structure of the proposed antenna. (a) Low band basic dipole. (b) High band basic dipole.

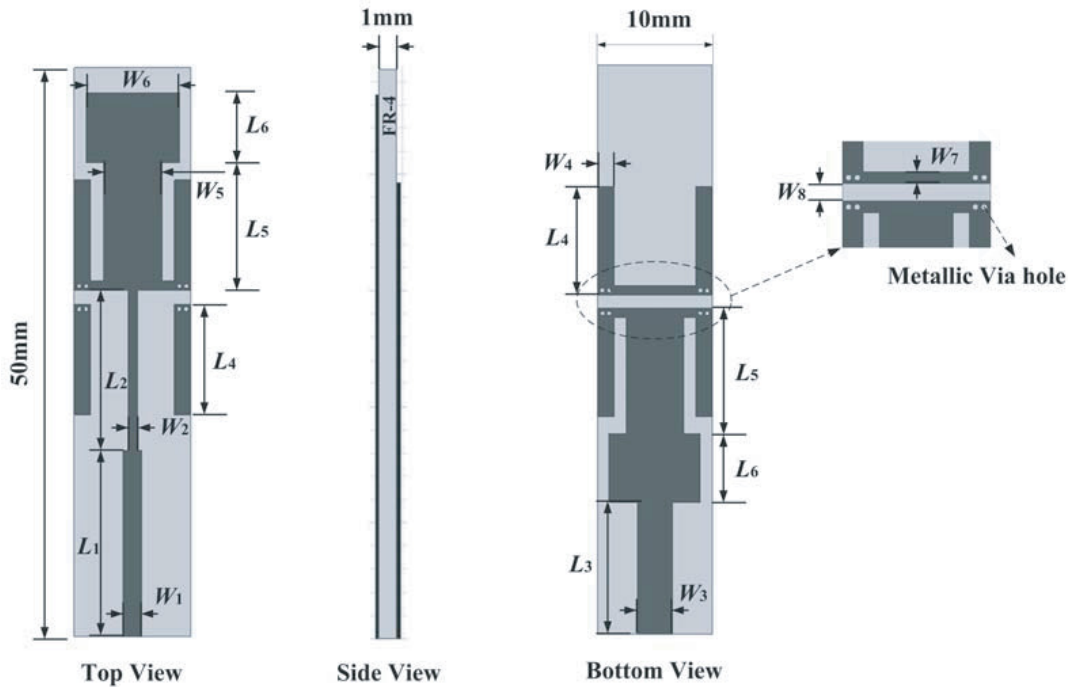


Figure 2. Geometry and configuration of the proposed antenna.

high band dipole consists of two half-wavelength dipoles arranged symmetrically along the axis. Figure 2 shows the geometry and configuration of the proposed antenna. As shown, the proposed antenna is mainly composed of two pairs of half-wavelength dipoles with different lengths. The longer dipole operating at lower band is printed in the middle of the structure, while the shorter one is printed on both sides of the structure. In order to obtain more stable radiation patterns and decrease the ellipticity, parasitical arms of the high band dipole are printed on the other side of the substrate and connected by metallic via holes. As depicted in Figure 2, these metallic via holes are only to ensure the electrical connection of the radiation arm and the parasitic arm on both sides, so there is no special requirement. Moreover, the width of the low band dipole is emboldened for wide band operation. As this dual-band omnidirectional antenna has single feed, a stair-stepping balun structure is added for impedance matching. An SMA connector is placed at the bottom to feed the antenna, in which the inner conductor is connected to the balun structure, while the outer conductor is connected to microstrip line with the width of W_3 . The proposed antenna is series-fed, and the input impedance should be transformed to 50Ω in order to match with SMA connector. Seen in Figure 2, the parallel two-wire transmission line has three parts with different widths (W_1 , W_2 , and W_3) and lengths (L_1 , L_2 , and L_3). By introducing the feeding structure and optimizing the above parameters, a distinct dual-band operation can be realized. The proposed antenna is printed on a low-cost FR4 substrate with thickness of 1 mm, relative dielectric constant of 4.4, and total size of $50 \text{ mm} \times 10 \text{ mm}$. This antenna is simulated and optimized with Ansoft HFSS which utilizes the Finite Element Method (FEM) for electromagnetic computation. Finally, we obtain the optimized antenna dimensions, as listed in Table 2.

Table 2. Dimensions of the proposed antenna (Unit: mm).

W_1	W_2	W_3	W_4	W_5	W_6	W_7
1.6	0.8	3	1.4	5	8	0.8
L_1	L_2	L_3	L_4	L_5	L_6	W_8
16	13.8	11.6	9.5	11	6	1.2

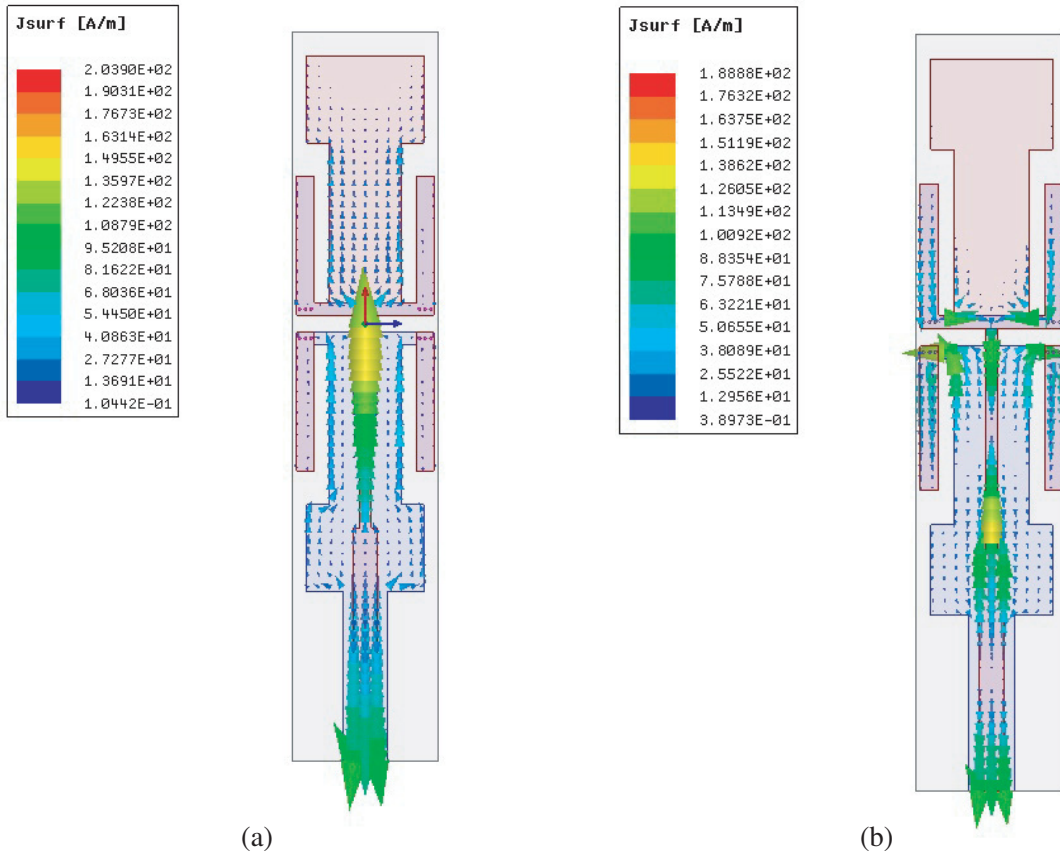


Figure 3. Current distributions of the proposed antenna. (a) 2.4 GHz. (b) 5.0 GHz.

To further study the dual-band operation mechanism, the current distributions on these two dipoles and balun structure are examined at 2.4 GHz and 5.0 GHz, as depicted in Figure 3. It can be seen that the current distributions are mainly centralized on the low band dipole when the dual-band antenna operates at 2.4 GHz, as shown in Figure 2(a). On the contrary, the current is mainly distributed on the high band dipoles at 5.0 GHz. Consequently, a dual-band operation is produced since these two dipole antennas operate at respective resonant frequencies. Moreover, the current flows along the dipoles, and the proposed dual-band antenna has realized vertical polarized radiation.

In order to provide readers with more information regarding the proposed antenna optimization and design, parametric studies have been conducted by simulation to investigate the effects of the key geometrical sizes on the impedance characteristics. Rigorous simulations indicate that the dual-band character and operation band are mainly determined by the width of balun structure (W_1), the length of the high band dipole arms (L_4), the width of the low band dipole arms (W_5), and the length of the turning stub (L_6). These parameters could be optimized to improve the impedance matching and realize the dual-band operation. To gain a good understanding of the influence of these parameters, only one parameter is investigated at a time, whereas the others are kept fixed. Based on the principle of half-wave dipole antenna, the operation frequency is mainly determined by the length of the dipole arms. As the proposed antenna is dual-band operation, the impedance matching is also affected by the balun structure. The results for the width of the balun structure (W_1) varied from 1.2 mm to 2.0 mm are presented in Figure 4. It is noted that the lower resonant frequency changes obviously with the width of the balun structure. When W_1 equals 1.6 mm, the simulated $|S_{11}|$ is below -10 dB within a wide frequency range.

The effect of high band dipole arms is also studied, as shown in Figure 5. It can be seen that the dual-band operation characteristics are strongly affected by the length of high band dipole arms (L_4). Furthermore, it indicates that with the increase of length, the high band resonant frequency shifts to

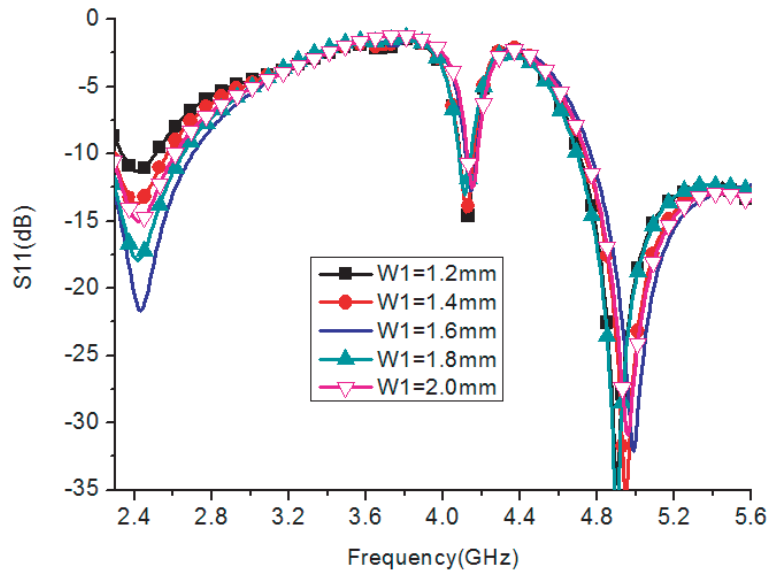


Figure 4. Simulated $|S_{11}|$ versus width of balun structure (W_1).

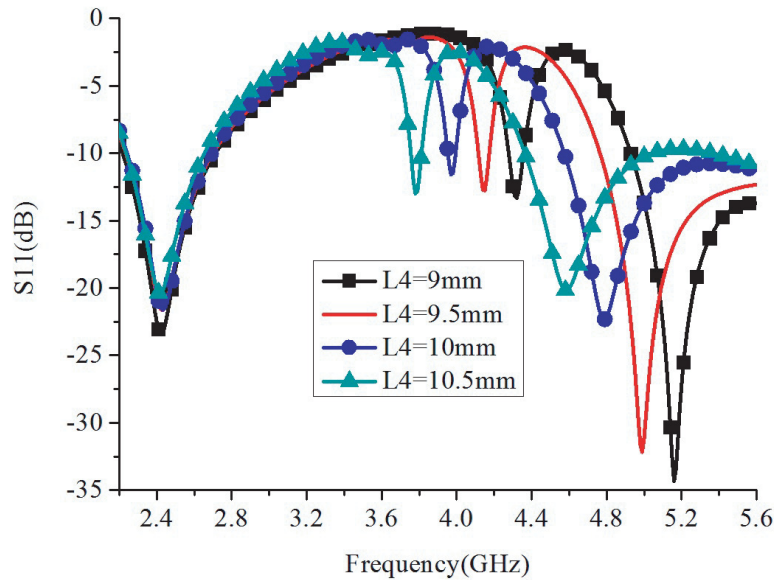


Figure 5. Simulated $|S_{11}|$ versus length of high band dipole arms (L_4).

lower band. Meanwhile, the impedance matching of the operation band is deteriorating. With this parameter adjusted precisely, the proposed antenna would operate at 5.0 GHz with good impedance matching.

The width of the low band dipole arms (W_5) is also one of the key parameters, which will affect the bandwidth of the low band operation. The results for W_5 varied from 4 to 6 mm are detailed in Figure 6. It is noted that the bandwidth of low band increases as the parameter W_5 decreases. Considering synthetically the influence on the high band operation, 5 mm is chosen for good impedance matching. The length of the turning stub (L_6) has a similar effect to the parameter of L_4 , which is depicted in Figure 7.

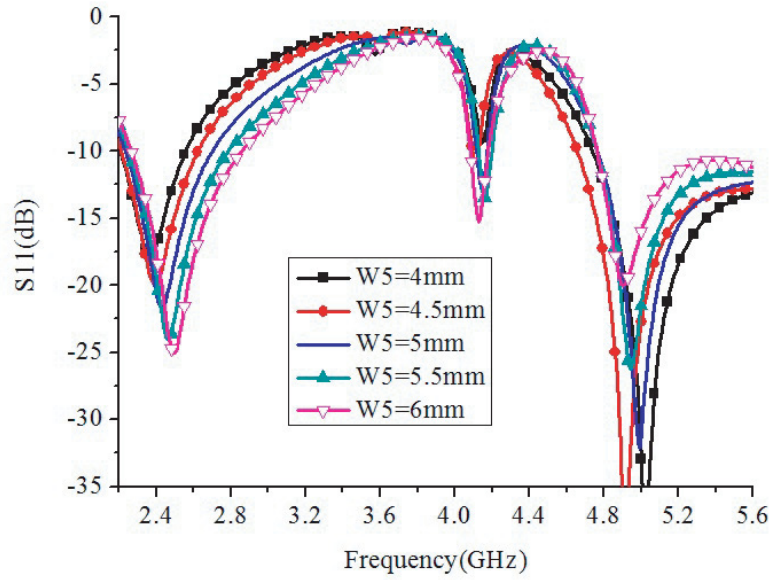


Figure 6. Simulated $|S_{11}|$ versus the width of low band dipole (W_5).

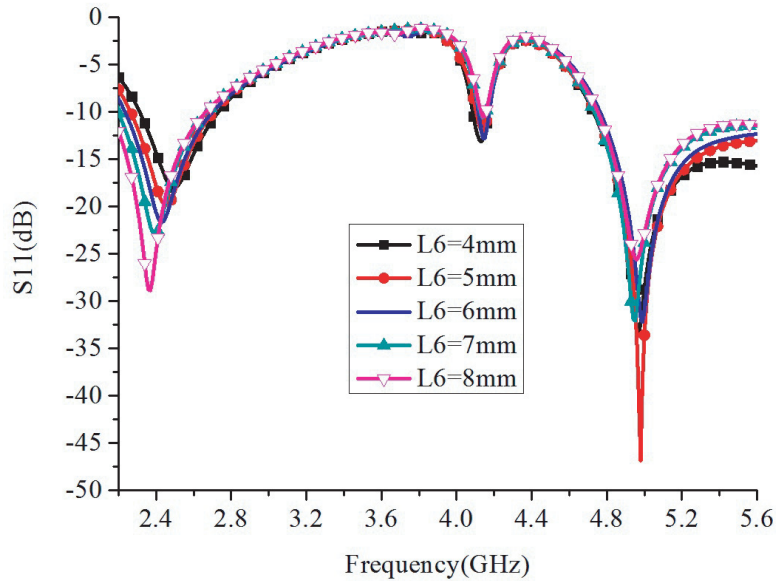


Figure 7. Simulated $|S_{11}|$ versus length of the turning stub (L_6).

3. RESULTS AND DISCUSSION

To verify the proposed design, a prototype of the antenna based on optimized dimensions has been fabricated, as shown in Figure 8. The reflection coefficient $|S_{11}|$ is measured with the Vector Network Analyzer, while the radiation pattern and gain are measured with the antenna far-field measurement system in an anechoic chamber. When the proposed dual-band antenna is under test, it works as a receiver and a horn antenna as the same operation band is used to transmit the signal.

The measured and simulated $|S_{11}|$ against frequency for the proposed antenna are plotted and compared in Figure 9. As shown in this figure, for $|S_{11}| \leq -10$ dB, the impedance bandwidth is approximately 19.2% ranging from 2.24 to 2.70 GHz centered at 2.4 GHz and over 17.4% ranging from

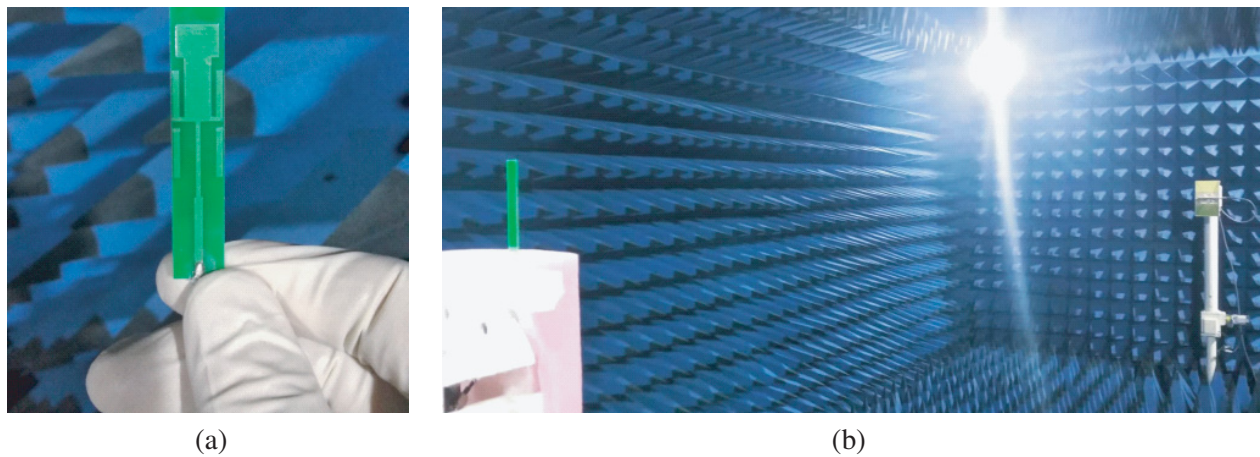


Figure 8. Photograph of the proposed antenna under test. (a) Photograph. (b) Antenna under test.

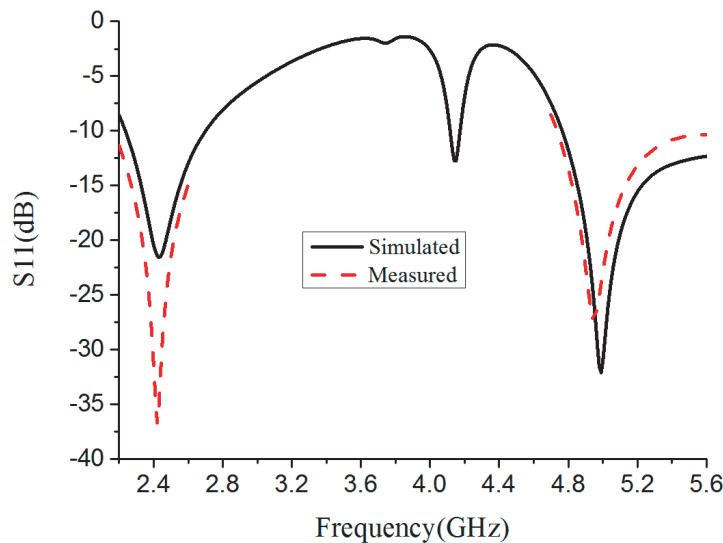


Figure 9. Simulated and measured $|S_{11}|$ against frequency.

4.73 to 5.6 GHz centered at 5.0 GHz. The discrepancy between the simulated and measured results can be mostly attributed to the measured environment effect and the tolerance in manufacturing.

We have also investigated the radiation characteristic of the proposed antenna in the far field. Figure 10 depicts the measured radiation patterns (*E* & *H* planes) of the designed omnidirectional antenna at 2.4 GHz and 5.0 GHz, respectively. As seen, the radiation patterns are normalized and show good axisymmetric properties. The beamwidth of *E* plane at 2.4 GHz is wider than that at 5.0 GHz. For the proposed omnidirectional antenna, the ellipticity of *H* plane is one of the key indicators. As presented, the measured ellipticity of 2.4 GHz and 5.0 GHz is 1.2 dB and 2.1 dB, respectively. From an overall view of these radiation patterns, the proposed antenna exhibits a nearly omnidirectional radiation pattern in the *H*-plane and a dipole-like radiation pattern in the *E*-plane. All these results indicate that the proposed antenna realizes good dual-band operation and omnidirectional radiation characteristics.

The simulated and measured peak gains on the azimuth plane against frequency are depicted in Figure 11. Throughout the operating band, the measured gain is varied from 2.09 dBi to 2.87 dBi, and the antenna gain with a variation of less than 1.0 dB is achieved. Thus, the antenna exhibits stable gain across the operation band.

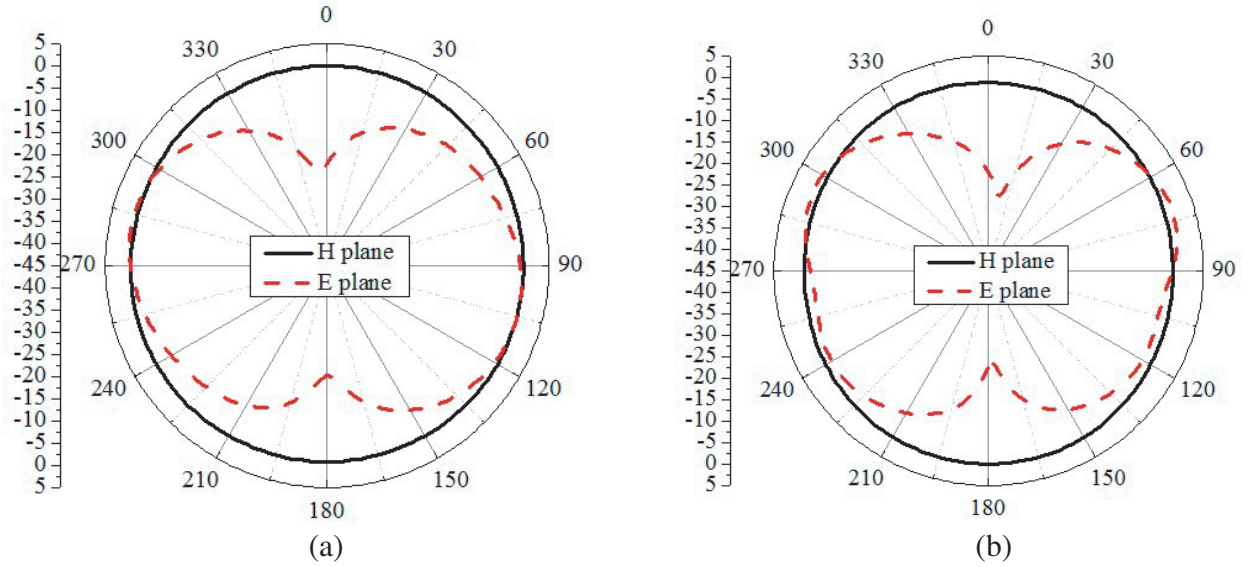


Figure 10. Measured normalized radiation patterns. (a) 2.4 GHz. (b) 5.0 GHz

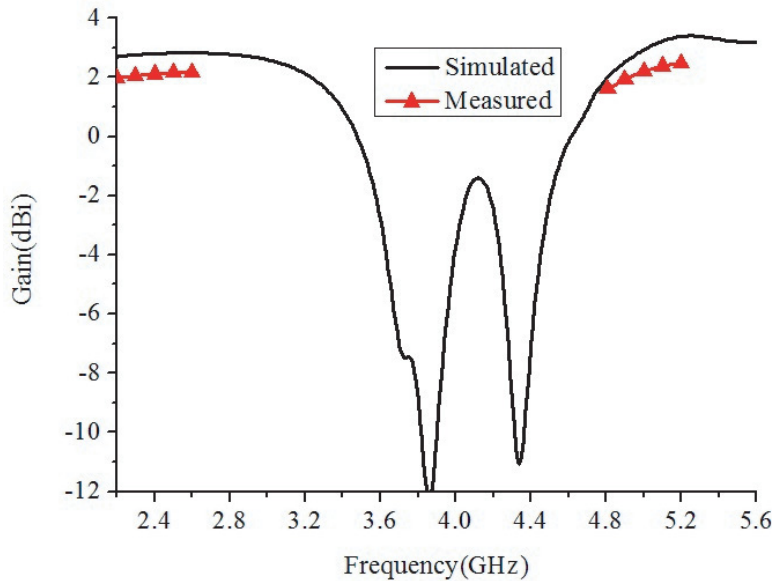


Figure 11. Simulated and measured peak gain against frequency.

4. CONCLUSION

A novel miniaturized dual-band omnidirectional antenna for WiFi applications has been proposed, investigated, and measured. A considerable miniaturized volume about $0.4\lambda_0 \times 0.08\lambda_0 \times 0.008\lambda_0$ is achieved. The simulated results are verified through the measured results, and a good agreement is achieved between the two. The proposed antenna achieves excellent impedance bandwidth of 19.2% (for 2.4 GHz band) and 17.4% (for 5.0 GHz band). Additionally, the measured peak gain of 2.09 ~ 2.87 dBi and ellipticity of 2.1 dB are obtained. These characteristics such as small volume, dual-band operation, and omnidirectional radiation patterns make this antenna as a potential candidate for the WiFi applications.

REFERENCES

1. Chen, Z. N., X. Qing, T. S. P. See, and W. K. Toh, "Antennas for WiFi connectivity," *Proceedings of the IEEE*, Vol. 100, No. 7, 2322–2329, 2012.
2. Zhang, B.-C., C. Jin, and Z.-X. Shen, "Low-profile broadband absorber based on multimode resistor-embedded metallic strips," *IEEE Trans. Microw. Theory Techn.*, Vol. 1, 1–9, 2019.
3. Lai, J., B. Feng, Q. Zeng, and S. Su, "A dual-band dual-polarized omnidirectional antenna for 2G/3G/LTE indoor system applications," *2018 IEEE International Conference on Signal Processing, Communications and Computing (ICSPCC)*, 2018.
4. Wen, H., Y. Qi, Z. Weng, F. Li, and J. Fan, "A multiband dual-polarized omnidirectional antenna for 2G/3G/LTE applications," *IEEE Antennas Wireless Propag. Lett.*, Vol. 17, No. 2, 180–183, 2018.
5. Guo, D., K. He, Y. Zhang, and M. Song, "A multiband dual-polarized omnidirectional antenna for indoor wireless communication systems," *IEEE Antennas Wireless Propag. Lett.*, Vol. 16, 290–293, 2017.
6. He, Y., K. Ma, N. Yan, and H. Zhang, "Dual band monopole antenna using substrate integrated suspended line technology for WLAN application," *IEEE Antennas Wireless Propag. Lett.*, Vol. 16, 2776–2779, 2017.
7. Liu, Y., X. Li, L. Yang, and Y. Liu, "A dual polarized dual band antenna with omnidirectional radiation patterns," *IEEE Trans. Antennas Propag.*, Vol. 65, No. 8, 4259–4262, 2017.
8. Hu, P. F., Y. M. Pan, K. W. Leung, and X. Y. Zhang, "Wide-/dual-band omnidirectional filtering dielectric resonator antennas," *IEEE Trans. Antennas Propag.*, Vol. 66, No. 5, 2622–2627, 2018.
9. Buckley, J. L., K. G. McCarthy, L. Loizou, B. O'Flynn, and C. O'Mathuna, "A dual-ISM-band antenna of small size using a spiral structure with parasitic element," *IEEE Antennas Wireless Propag. Lett.*, Vol. 15, 630–633, 2016.
10. Shi, W., Z. Qian, and W. Ni, "Dual-band stacked annular slot/patch antenna for omnidirectional radiation," *IEEE Antennas Wireless Propag. Lett.*, Vol. 15, 390–393, 2016.